Effect of Wavy Interface on Natural Convection in Square Cavity Partially Filled with Nanofluid and Porous Medium using Buongiorno Model

CHERIFA BENYGZER[1], MOHAMED BOUZIT[1], ABDERRAHEM MOKHEFI[2]
[1]LSIM Maritime Science and Engineering Laboratory, Faculty of Mechanical Engineering, Mohamed Boudiaf University of Science and Technology, El Maouar, Bp 1505, Bir Eldjir 31000, Oran,
ALGERIA

[2]L2ME Modeling and Experimentation Laboratory, Faculty of Sciences and Technology, Bechar University B.P.417, 08000, Bechar,
ALGERIA

Abstract: - Convective heat transfer improvement from wavy surfaces presents a new solution in industrial engineering for composite materials, including porous medium, and nanofluids to address the wavy irregular surfaces in heat transfer devices such as a wavy solar collector, energy absorption and filtration, thermal insulation, and geothermal power plants. This technique enables the performance of engineering applications. The numerical study is performed to examine the effects of a wavy interface separating two layers in the enclosure on heat exchange rates. This paper investigates numerically the natural convection flow in a square cavity partially filled with nanofluid-porous layers separated by a wavy horizontal interface. The left and right walls of the cavity are maintained at constant hot and cold temperatures, whereas the other walls are adiabatic. The Buongiorno model is used to describe nanofluid motion, taking into account the brownian and thermophoresis effects in the cavity. The Galerkin finite element method was applied to solve the differential governing equations. The dynamic, thermal field and heat transfer have been analyzed for various parameters such as Rayleigh number ($10^3 \leq Ra \leq 10^6$), the amplitude of interface ($0 \leq A \leq 0.1$), and undulation number ($0 \leq n \leq 9$). The results reveal that the flow intensity induced by buoyancy forces is more significant in the nanofluid layer than in the porous layer, since the heat transfer is enhanced while the flow is not sensitive to variations in amplitude and number undulation, and accordingly, the decline of average Nusselt and Sherwood numbers is insignificant. The effects of controlled parameters on the structure of nanofluid flow, heat, and mass transfer rate are insignificant.

Key-Words: - Wavy interface, nanofluid, heat transfer, Buongiorno model, natural convection, porous medium, layers, amplitude, undulation number, Galerkin finite element method.

Received: June 14, 2023. Revised: February 26, 2024. Accepted: April 11, 2024. Published: June 4, 2024.

1 Introduction

To improve the thermal conductivity of fluids, scientific research has multiplied in recent years and has made it possible to synthesize nano-sized particles dispersed in the base fluid, which constitute nanofluids used in several fields such as biochemistry and the oil industry.

The applications of nanofluids in thermal systems filled with porous medium and of different geometries, flow regimes, boundary conditions, and different types of nanofluids and thermophysical properties. Many researchers have investigated the nanofluids used in porous media due to their thermal characteristics.

The addition of nanoparticles to the pure fluid enhances considerably the heat transfer in the enclosure, [1], [2], [3], [4], [5], [6].

Also, the authors of [7], [8], [9], [10], [11], [12], [13], [14], [15], use hybrid nanofluids, which significantly improve the dynamic viscosity and thermal conductivity of the base fluid.

The horizontal and vertical orientation of the porous layer in the enclosure was reported, [16], [17], [18], [19].

The natural convection in the wavy cavity-saturated Cu-water nanofluid has been studied by some authors, [20], [21], they examined the effect of the Rayleigh number, the wave amplitude, and the

undulations number on the heat transfer rate, the amplitude ratio was found to be significant in the rise of the heat transfer in a porous cavity with sinusoidal heating on both sidewalls, [22], therefore the convective flow is attenuated with growth of undulation under the effect of thermal dispersion [23], while the wave number can control the free convective motion and heat transport within the wavy cavity, [24]. Thus, the heat transfer rates were sensitive to the variation of undulation property, convection intensity, [25].

The choice of different fluids has been the subject of some authors. The paper [26] investigates the effect of the sinusoidal interface on the heat and mass transfer of laminar clear fluid and porous medium.

The nanofluid is modeled using Buongiorno's model, incorporating thermophoresis and Brownian motion effects, [27]. We cite in the literature a numerical study of natural convection inside a porous, wavy cavity filled with a nanofluid using the Forchheimer-Buongiorno approach, [23].

Laminar natural-convective flow in a square composite vertically layered enclosure consisting of porous and nanofluid layers separated by a sinusoidal corrugated interface has been reported by [28], they found that the increase in Darcy's number of porous media with a low value of the non-uniform porous layer thickness enhances the convective heat transfer in the cavity. On the other hand, a decrease in the Darcy parameter brings a big resistance force for the fluid flow and an increase in heat transfer by conduction, [29], [30].

The heat transfer increases with the increase of modified Rayleigh number, volume fraction, and amplitude in a porous square cavity saturated by a nanofluid (Al_2O_3-Water) in the presence of a corrugated heat source, [31].

In addition, the heat transfer rates through the nanofluid and solid phases are found to be better for high values of the undulation amplitude, [32].

The impacts of various effective parameters, which include nanoparticle volume fraction, Darcy number, modified conductivity ratio, the number of undulations, and the amplitude, on the heat transfer rate in a wavy-walled porous enclosure are being analyzed, [33].

The study of natural convection in a two-dimensional enclosure with horizontal wavy walls layered by a porous medium, saturated by Cu-Al2O3/water hybrid nanofluid has been performed in [34].

The increase in porous layer width leads to a decline in the average Nusselt and Sherwood numbers in a square cavity filled with power-law fluid and porous media separated by a wavy interface, [35]. The studies of [36], [37], [38] reported the natural convection in a square enclosure divided by a corrugated porous partition, either horizontally or vertically, in porous and fluid regions and a porous cavity filled with a hybrid nanofluid and non-newtonian layers. Higher amplitude and the undulation number of the sinusoidal interface between the nanofluid and porous medium layer lead to a decrease in the average Nusselt number of natural convection in a square cavity filled by a nanofluid (Cu-water) /porous-medium, [39].

In this paper, a numerical investigation of the natural convection in a square cavity partially filled with porous and nanofluid separated by wavy was performed. The effects of amplitude, undulation number of the interface on the dynamic and thermal fields, heat, and mass transfer rate are analyzed for various values.

In reviewing the literature, we found no published work for composite porous cavities saturated with nanofluid flow modeled using the Buongiorno model.

This work provides an original contribution: to develop high-performance materials with minimum power consumption for future industrial applications.

2 Physical Model

The configuration considered in the present study is shown in Figure 1. The physical domain consists of a 2D square cavity heated from the left vertical wall and cold from the right wall at constant temperatures T_h and T_c, respectively. The horizontal walls are considered adiabatic. This cavity is filled with a nanofluid and porous layer separated by a horizontal, wavy interface. The nanofluid occupies the lower part, and the porous medium is placed above the mid-plane of the cavity.

- H is the height of the cavity.
- H/2 is the width of the porous and nanofluid layers.
- The fluid flow is considered to be laminar and incompressible, and the porous medium is assumed to be homogenous and isotropic.
- The constant thermophysical properties of water and nanofluids at 25^{o}C are given in Table 1.

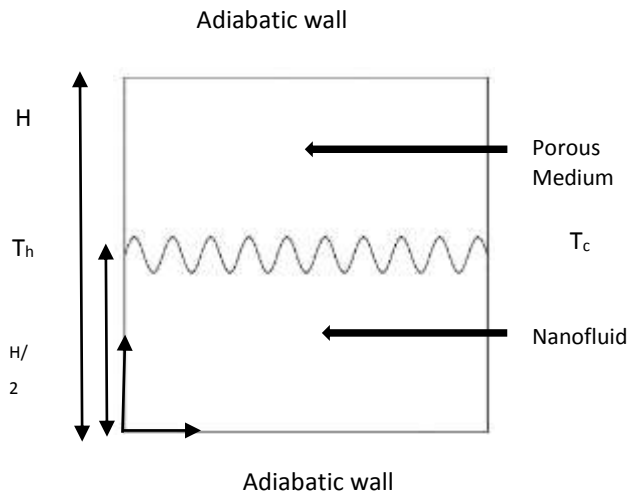

Fig. 1: Physical model

Table 1. Thermophysical properties of water

Physical property	Water
C_p (J/kg K)	4179
ρ (kg /m^3)	997.1
k (W/m .K)	0.613
B (K^{-1})	21e-5
μ (kg/m s)	8.55e-4

2.1 Mathematic Model

The two-dimensional equations governing the stationary flow of nanofluid in natural convection inside a square cavity using the Buongiorno mathematical model are described as follows:

$$\frac{\partial \rho}{\partial t}+\rho_f\left(\frac{\partial u}{\partial x}+\frac{\partial v}{\partial y}\right)=0 \tag{1}$$

$$\rho_f\left(\frac{\partial u}{\partial t}+u\frac{\partial u}{\partial x}+v\frac{\partial u}{\partial y}\right)=-\frac{\partial p}{\partial x}+\mu_f\left(\frac{\partial^2 u}{\partial x^2}+\frac{\partial^2 u}{\partial y^2}\right)-\frac{\mu}{K}u \tag{2}$$

$$\rho_f\left(\frac{\partial v}{\partial t}+u\frac{\partial v}{\partial x}+v\frac{\partial v}{\partial y}\right)=-\frac{\partial p}{\partial y}+\mu_f\left(\frac{\partial^2 v}{\partial x^2}+\frac{\partial^2 v}{\partial y^2}\right)-\frac{\mu}{K}v$$
$$+\left[(1-C_c)\rho_f(T-T_c)\beta_f-(C-C_c)(\rho_s-\rho_f)\right]g \tag{3}$$

$$\frac{\partial T}{\partial t}+u\frac{\partial T}{\partial x}+v\frac{\partial T}{\partial y}=\alpha\left(\frac{\partial^2 T}{\partial x^2}+\frac{\partial^2 T}{\partial y^2}\right)$$
$$+\delta\left\{D_B\left(\frac{\partial T}{\partial x}\frac{\partial C}{\partial x}+\frac{\partial T}{\partial y}\frac{\partial C}{\partial y}\right)+\frac{D_T}{D_C}\left[\left(\frac{\partial T}{\partial x}\right)^2+\left(\frac{\partial T}{\partial y}\right)^2\right]\right\} \tag{4}$$

$$\frac{\partial C}{\partial t}+u\frac{\partial C}{\partial x}+v\frac{\partial C}{\partial y}=D_B\left(\frac{\partial^2 C}{\partial x^2}+\frac{\partial^2 C}{\partial y^2}\right)+\frac{D_T}{D_C}\left(\frac{\partial^2 T}{\partial x^2}+\frac{\partial^2 T}{\partial y^2}\right) \tag{5}$$

$$D_B=\frac{K_B T_0}{3\pi d_b \mu} \tag{6}$$

$$D_B=\frac{K_B T_0}{3\pi d_b \mu} \tag{7}$$

The continuity, momentum, and energy equations can be written in dimensionless form as follows by introducing dimensionless variables:
The flow is assumed to be stationary and incompressible.

$$(X,Y)=\frac{(x,y)}{H},(U,V)=\frac{H(u,v)}{\alpha_f},\theta=\frac{T-T_c}{T_h-T_c},\varphi=\frac{C-C_C}{C_h-C_c},P=\frac{pH^2}{\rho_f\alpha^2{}_f} \tag{8}$$

$$\frac{\partial U}{\partial X}+\frac{\partial V}{\partial Y}=0 \tag{9}$$

$$U\frac{\partial U}{\partial X}+V\frac{\partial U}{\partial Y}=-\frac{\partial P}{\partial X}+\Pr\left(\frac{\partial^2 U}{\partial X^2}+\frac{\partial^2 U}{\partial Y^2}\right)-\frac{\Pr}{Da}U \tag{10}$$

$$U\frac{\partial V}{\partial X}+V\frac{\partial V}{\partial Y}=-\frac{\partial P}{\partial Y}+\Pr\left(\frac{\partial^2 V}{\partial X^2}+\frac{\partial^2 V}{\partial Y^2}\right)-\frac{\Pr}{Da}V+Ra\Pr(\theta-Nr\varphi) \tag{11}$$

$$U\frac{\partial \theta}{\partial X}+V\frac{\partial \theta}{\partial Y}=\frac{\partial^2 \theta}{\partial X^2}+\frac{\partial^2 \theta}{\partial Y^2}$$
$$+Nb\left(\frac{\partial \theta}{\partial X}\frac{\partial \varphi}{\partial X}+\frac{\partial \theta}{\partial Y}\frac{\partial \varphi}{\partial Y}\right)+Nt\left[\left(\frac{\partial \theta}{\partial X}\right)^2+\left(\frac{\partial \theta}{\partial Y}\right)^2\right] \tag{12}$$

$$U\frac{\partial \varphi}{\partial X}+V\frac{\partial \varphi}{\partial Y}=\frac{1}{Le}\left(\frac{\partial^2 \varphi}{\partial X^2}+\frac{\partial^2 \varphi}{\partial Y^2}\right)+\frac{Nt}{LeNb}\left(\frac{\partial^2 \theta}{\partial X^2}+\frac{\partial^2 \theta}{\partial Y^2}\right) \tag{13}$$

New parameters appear in the dimensionless equations: Prandtl number, Darcy number, Rayleigh number, buoyancy ratio, Brownian motion, thermophoresis and Lewis number.

$$\Pr=\frac{\mu Cp}{k} \tag{14}$$

$$Da=\frac{K}{H^2} \tag{15}$$

$$Ra=\frac{(1-C_c)\beta_f g(T_h-T_c)H^3}{\nu_f \alpha_f} \tag{16}$$

$$Nr=\frac{(C_h-C_c)(\rho_s-\rho_f)}{(1-C_c)\beta_f \rho_f (T_h-T_c)} \tag{17}$$

$$N_B=\frac{(C_h-C_c)D_B(\rho Cp)_s}{\alpha_f(\rho Cp)_f} \tag{18}$$

$$N_T=\frac{D_T}{T_c}\frac{(\rho Cp)_s}{(\rho Cp)_f}\frac{(T_h-T_c)}{\alpha_f} \tag{19}$$

$$Le=\frac{\alpha_f}{D_B} \tag{20}$$

The physical quantities of heat transfer are local, average Nusselt and Sherwood numbers respectively Nu $_{loc}$, Sh $_{loc}$, Nu $_{avg}$, Sh $_{avg}$ are defined as below:

$$Nu_L = -\left.\frac{\partial\theta}{\partial X}\right|_{X=1}, Sh_L = -\left.\frac{\partial\varphi}{\partial X}\right|_{X=1} \quad (21)$$

$$Nu_{avg} = \int_0^1 -\frac{\partial\theta}{\partial X}dY, Sh_{avg} = \int_0^1 -\frac{\partial\varphi}{\partial X}dY \quad (22)$$

2.2 Boundary Conditions

The proposed problem provides a boundary condition in the dimensionless form of the cavity walls:

At X = 0, $0 \le Y \le 1$ U, V = 0 $\theta = \varphi = 1$ and $Nt\frac{\partial\theta}{\partial X} + Nb\frac{\partial\varphi}{\partial X} = 0$

At X = 1, $0 \le Y \le 1$ U, V = 0 $\theta = \varphi = 0$ and $Nt\frac{\partial\theta}{\partial X} + Nb\frac{\partial\varphi}{\partial X} = 0$

At Y = 0, 1 and $0 \le Y \le 1$ U = V = 0 , $\frac{\partial\theta}{\partial Y} = 0$, $\frac{\partial\varphi}{\partial Y} = 0$

The continuity conditions at the sinusoidal horizontal interface are described as follows:

$$U|_p = U|_{nf}, V|_p = V|_{nf}, P|_p = P|_{nf}, \theta|_p = \theta|_{nf}, \left.\frac{\partial\theta}{\partial n}\right|_{nf} = \frac{k_{nf}}{k_f}\left.\frac{\partial\theta}{\partial n}\right|_p$$

$$C|_p = C|_{nf}, \left.\frac{\partial C}{\partial n}\right|_{nf} = \frac{\alpha_{nf}}{\alpha_f}\left.\frac{\partial C}{\partial n}\right|_p$$

3 Numerical Method and Validation

The finite element method is applied to discretize the dimensionless partial differential equations provided in Eqs. (9) to (13) that are associated with the boundary conditions based on the Galerkin scheme. The convergence criterion is 1e-6 for each variable.

3.1 Grid Independence Test Mesh

A 2D triangular mesh was generated to cover the computational domain of the considered configuration with 82268 elements.

A grid independence test series was proposed in this study to select the optimum grid size with the following number of elements: 51104, 55786, 62634, 82268, and 111136 to determine the appropriate study mesh size (Table 2).

Figures 2 (a) and (b) show the meshes of the studied configuration; the interface line between the porous and nanofluid layers was refined to capture the flow behaviors.

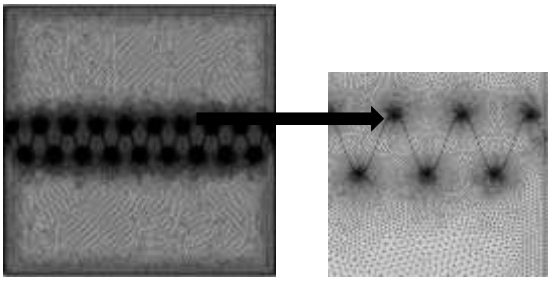

(a) (b)

Fig. 2: Computational mesh of the physical domain (a), (b) refined mesh of the interface line

Table 2. Independence test of mesh

E Nr	51104	55786	62634	**82268**	111136
Time	31608 s	30276 s	2686 s	**9435 s**	44345 s
ψ_{max}	5.17445	5.17570	5.17647	**5.17727**	5.17761
θ_{avg}	0.59358	0.59360	0.59361	**0.59362**	0.59362
φ_{avg}	1.02117	0.98350	0.97116	**0.95820**	0.95366
Nu $_{avg}$	3.54361	3.54496	3.54575	**3.54652**	3.54687
Sh $_{avg}$	3.54363	3.54497	3.54575	**3.54652**	3.54688

Five numbers of elements are compared to check the mesh independence at Ra = 10^5, Da = 10^{-3}, Pr =5.82, A = 0.05, n = 9, and Le = Nt = Nb = Nr = 0.1. The deviations of Nu $_{avg}$ and Sh $_{avg}$ between the grids G4 and G5 are very small. The gird G4 seems to be the most suitable for this study.

3.2 Validation

The results of the present study for average Nusselt number variation with volume fraction Al_2O_3 nanoparticles are compared with those of [40], investigating heat transfer convective in a square cavity .

The validation plot (Figure 3) was completed under identical conditions, and both the previous studies' findings are in good agreement. The error of the average Nusselt number value is estimated at 2.03% for the Darcy number value 10^{-3} as shown in Table 3.

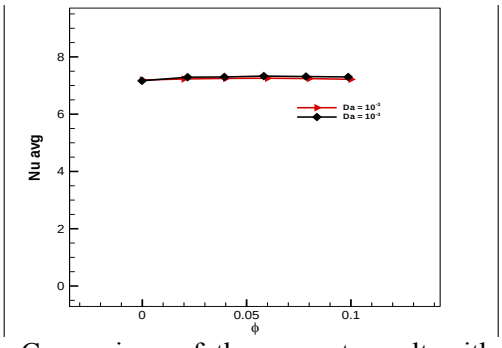

Fig. 3: Comparison of the present result with the numerical results of [40]

Table 3. Validation of average Nusselt number values

Da	Ra	Sheikhzadeh et al (2013)	Present study	Error %
10^{-3}	10^{-5}	7.25	7.40	2.03

4 Results and Discussions

The main interest in this study is focused on the effect of the horizontal wavy interface on the structure of the flow in the partially filled cavity with nanofluid and porous medium. The results of the different numerical simulations are presented by streamlines, isotherms, and iso-concentration contours, as well as local, average Nusselt and Sherwood numbers.

The simulations are performed for the fixed values of Rayleigh number Ra = 10^5, Darcy number Da = 10^{-3}, the dimensionless amplitude of interface A = 0.05, undulation number n = 9, Lewis number Le, buoyancy ratio Nr, brownian motion Nb, thermophoresis parameter Nt and Le = Nt = Nb = Nr = 0.1.

The results will consecutively present the effect of various values of the Rayleigh number ($10^3 \leq Ra \leq 10^6$), the dimensionless amplitude ($0 \leq A \leq 0.1$), and the undulations number ($0 \leq n \leq 9$).

4.1 Effect of Rayleigh Number

Figure 4 represents the distribution of streamlines, isotherms, and iso-concentrations for various values of the Rayleigh number ($10^3 \leq Ra \leq 10^6$).

For a low Rayleigh number (Ra = 10^3), the main cell circulation is located on the nanofluid portion of the cavity and rotates clockwise;the flow is immobile in the porous portion.

In the porous layer, temperature and concentration gradients are weak, indicating a conductive flow [30].

The cell circulation is intensified by increasing the Rayleigh number from Ra = 10^4 to 10^5.

The cell circulation is elongated horizontally and is still located on the nanofluid layer, It is noticed that at Ra = 10^6, the infiltration of nanofluid is detected in the porous layer « By increasing the Ra number, remarkable penetration in the direction of the porous layer is detected, due to the elongation of the main vortex » [35].

Streamline intensity indicates that a high-temperature gradient contributes to enhancing heat transfer and the dominance of convective heat transfer« Streamlines shown at Ra = 10^5 and 10^7 indicate that the fluid circulation strength becomes higher when the mode of heat transfer is transferred from conduction to convection with more vortices and distortion in the flow pattern [36].

The isotherms and iso-concentrations are parallel to the vertical wall at Ra = 10^3, denoting the conductive heat transfer in the porous and nanofluid layers.

By increasing Rayleigh's number from Ra = 10^4 to 10^6, isotherm lines become horizontal and very dense close to the left hot wall into the nanofluid layer. In the porous layer, they remain diagonal.

A high-temperature gradient was observed due to the convective heat exchange. The flow passes from a conductive to a convective regime by increasing the Ra number [30].

Iso concentrations are modified to a horizontal shape by increasing Ra =10^5 in both layers. At Ra =10^6, an important nanoparticle concentration is observed near the hot left wall, signifying important convective heat transfer.

The distribution of streamlines, isotherms, and iso-concentrations confirms that the strength of flow is more significant in the nanofluid layer than in the porous layer« The intensity of circulation is always much stronger in the fluid region than in the porous region. The magnitude of penetration of flow from the fluid region to the porous region is substantially influenced by the Rayleigh number » [37].

High buoyancy forces reinforce nanofluid circulation in the cavity and consequently, convective transfer is enhanced.

4.2 Effect of Dimensionless Amplitude

Figure 5 shows the effect of the various values of dimensionless amplitude ($0 \leq A \leq 0.1$) on the streamlines, isotherms, and iso-concentrations contours.

By increasing the amplitude of interface A from 0 to 0.05, the cell circulation intensity does not change; the flow is located in the nanofluid layer, while the flow in the porous region is immobile; indeed, the convection dominates the flow. The streamline intensity decreases slightly from A = 0.075 to 0.1. The flow is not sensitive to variations in dimensionless amplitude.

Isotherms are horizontal in the nanofluid layer due to the dominance of convection mode; in the porous layer, their shape is diagonal.

Iso-concentrations are completely stratified at the bottom cavity; we explain this phenomenon by nanoparticle concentrations due to the thermophoretic force effect.

The dimensionless amplitude effect is not significant for nanofluid circulation, temperature, or concentration of nanoparticles.

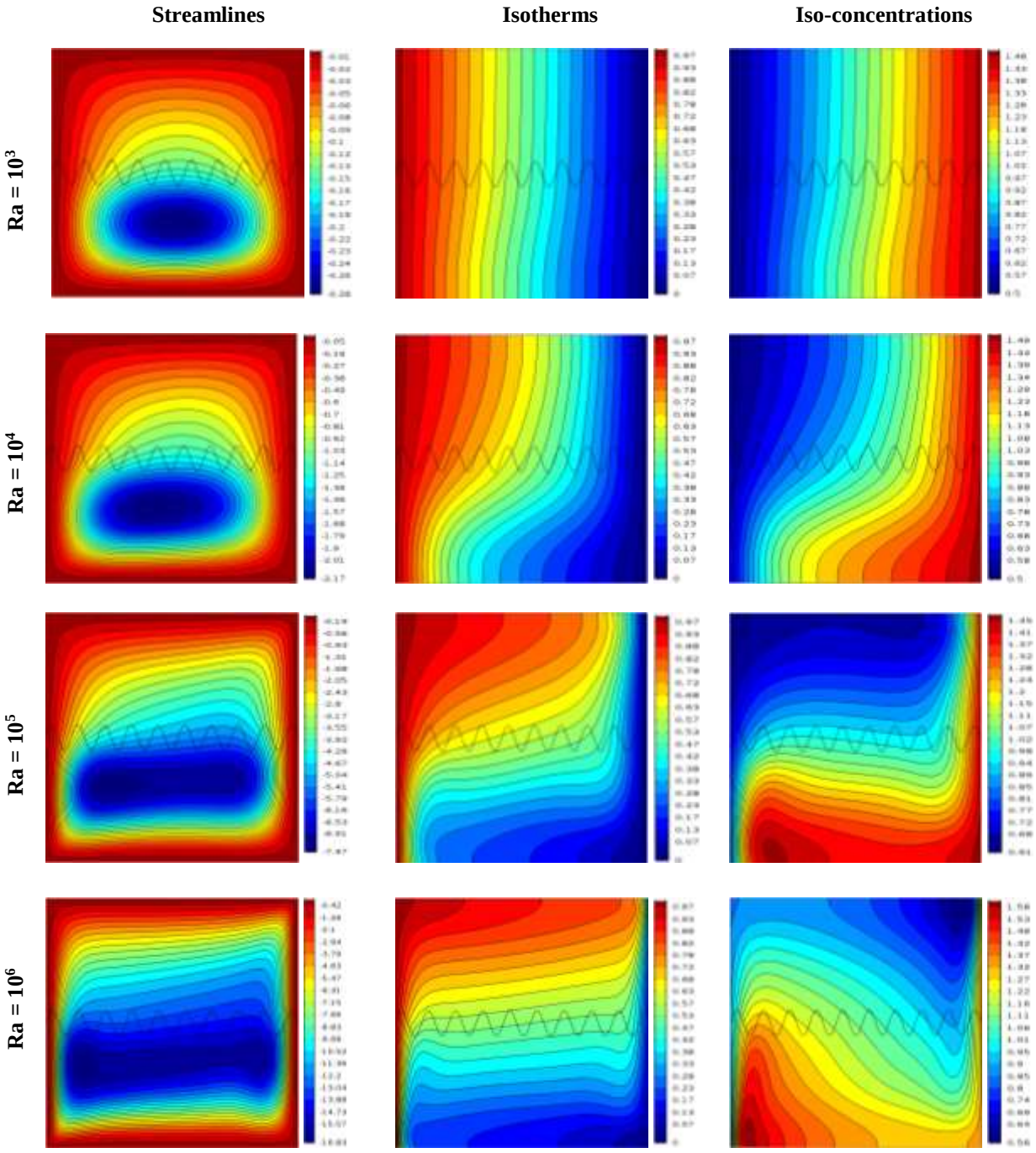

Fig. 4: Variation of Ra on streamlines, isotherms and iso-concentrations, A = 0.05, n = 0.9, Da = 10^{-3}, Le = Nr = Nb = Nt = 0.1

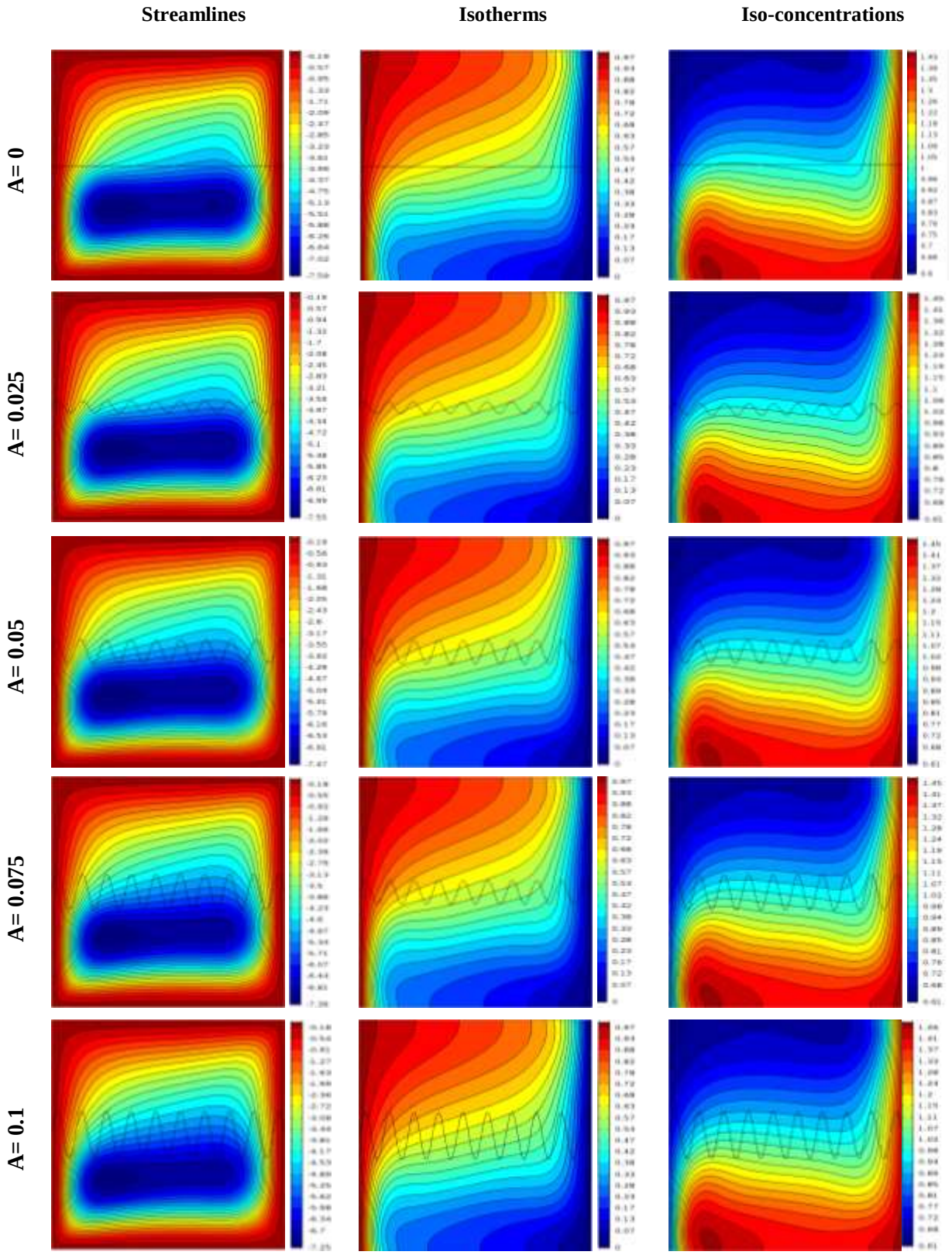

Fig. 5: Variation of A on streamlines, isotherms and iso-concentrations , Ra =10^5, Da = 10^{-3}, n = 0.9 , Da = 10^{-3}, Le = Nr = Nb = Nt = 0.1

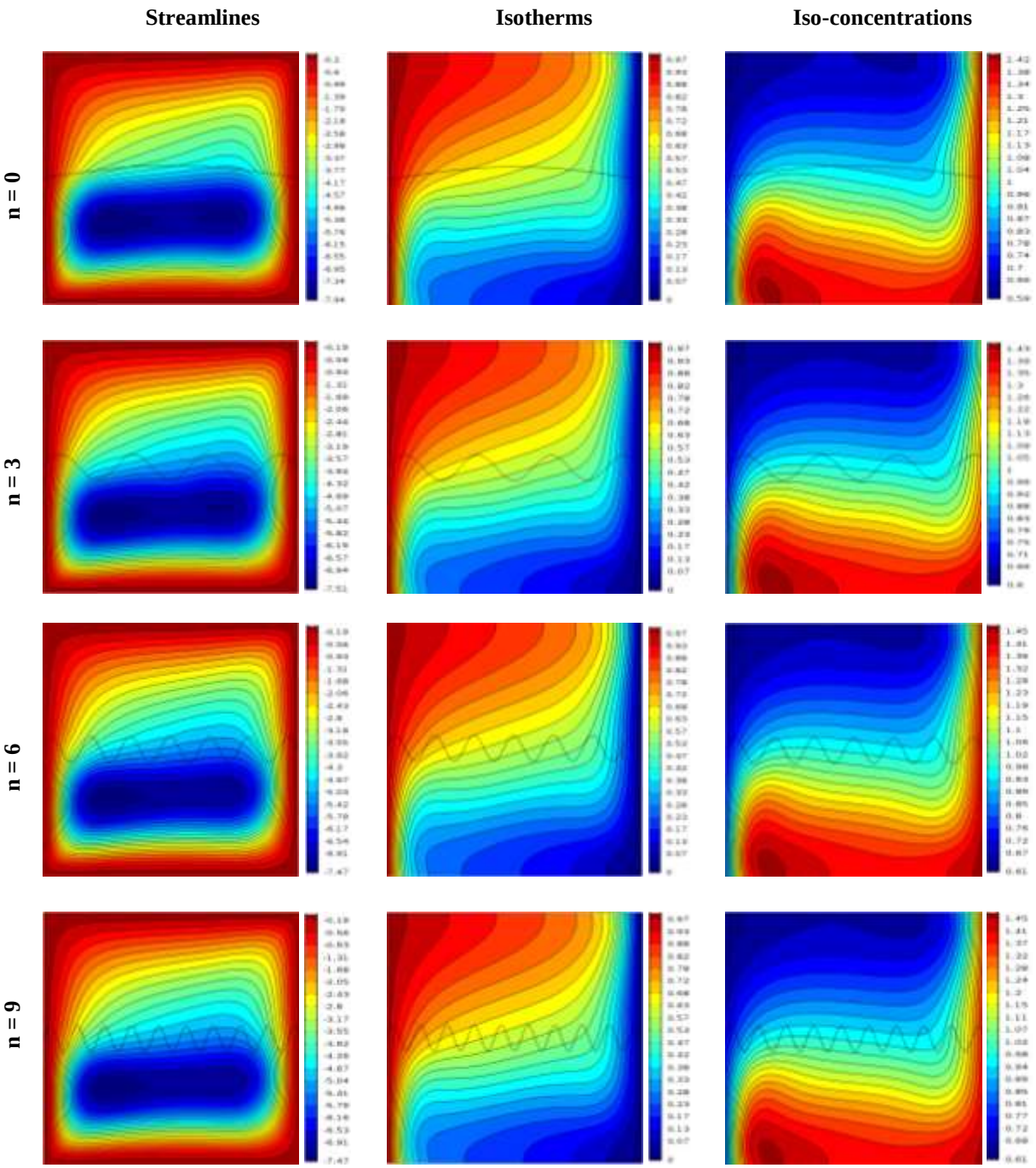

Fig. 6: Variation of n on streamlines, isotherms and iso-concentrations $Ra = 10^5$, $Da = 10^{-3}$, $A = 0.05$, $Da = 10^{-3}$, $Le = Nr = Nb = Nt = 0.1$

4.3 Effect of the Undulation Number

Figure 6 represents the distribution of the streamlines, the isotherms, and the iso-concentrations for various values of the undulation number ($0 \leq n \leq 9$).

It is observed that the intensity of the cell circulation does not change, whatever the increase in the undulation number. The heat transfer is convective.

The isotherm lines are diagonal in the porous layer, while in the nanofluid layer, the isotherms are horizontal to the left hot wall and become denser, indicating the convection mode.

The iso-concentration stratification zone was detected in the nanofluid layer, which means a high nanoparticle concentration near the hot left wall due to the thermophoresis effect.

The undulation number doesn't influence the dynamic and thermal fields.

4.4 Compute of local, Average Nusselt and Sherwood numbers

Figure 7, Figure 8, Figure 9, Figure 10, Figure 11 and Figure 12 represent the evolution of the local, average Nusselt and Sherwood d numbers along the left hot wall as a function of Y coordinate for various values of Rayleigh number ($10^3 \leq Ra \leq 10^6$), dimensionless amplitude ($0 \leq A \leq 0.1$) and undulation number ($0 \leq n \leq 9$).

4.4.1 Impact of the Rayleigh number

Figure 7 represents the variation of the local Nusselt Nu_{loc} (a) and Sherwood Sh_{loc} (b) numbers for various values of the Rayleigh number ($10^3 \leq Ra \leq 10^6$).

In Figure 7 (a) and (b), it is observed that the high values of local Nusselt and Sherwood numbers are obtained at the bottom of the hot left wall ($Y = 0$) and decrease by moving along the height of the hot left wall at $Y = 1$.

A high increase in local Nusselt and Sherwood numbers from $Ra = 10^5$ to 10^6 was marked « It is noticeable that the local Nu intensifies significantly from $Ra = 10^5$ to 10^6» [38]; this increase is less important from $Ra = 10^3$ to10^4 due to the lower heat and mass exchange between the porous and nanofluid layers, where conduction dominates in the cavity.

Figure 8 shows the variation of average Nusselt and Sherwood numbers with Rayleigh number from $Ra = 10^3$ to 10^6. At low Rayleigh number $Ra = 10^3$ to 10^4, an insignificant increase in Nu_{avg} and Sh_{avg} was noticed due to the conductive regime, while for higher Rayleigh number from 10^5 to 10^6, this increase is more significant.

Higher values of average Nusselt and Sherwood numbers are interpreted by the dominance of convection.

A significant heat and mass transfer occurred due to increasing buoyancy forces.

Variations in Rayleigh number values indicate the same heat and mass transfer rate.

4.4.2 Impact of Dimensionless Amplitude

Figure 10 (a) and (b) illustrate the evolution of the local Nusselt and Sherwood numbers according to the value of the dimensionless amplitude ($0 \leq A \leq 0.1$).

It is clear that the increase in amplitude A does not influence the local Nusselt and Sherwood numbers curves in the porous layer, however a slight decline was observed in the nanofluid layer when A increased for the two numbers.

Figure 9 shows the evolution of the average Nusselt and Sherwood numbers as a function of amplitude A. It is noticed that Nu_{avg} and Sh_{avg} decrease linearly as the amplitude increases « higher amplitude and the undulation number of the sinusoidal interface between the nanofluid and porous medium layer lead to a decrease in the average Nusselt number», [39].

The decrease of Nu_{avg} and Sh_{avg} is not significant, which is reflected in a low rate of heat and mass transfer.

Heat and mass transfer are not sensitive to the change in amplitude.

The amplitude of wavy interface variation provides the same rate of heat and mass transfer.

4.4.3 Impact of the Undulation Number

Figure 11 (a) and (b) demonstrate the variation of local Nusselt and Sherwood numbers for various undulation numbers ($0 \leq n \leq 9$).

In Figure 11 (a) and (b), the Nu_{loc} and Sh_{loc} decrease slightly by increasing the undulation number n in the nanofluid layer «The average Nusselt number decreases by increasing the undulation number» [34], while in the porous layer, the increase of n does not change the value of the Nu_{loc} and Sh_{loc}.

Undulation number increase has no impact on local Nusselt and Sherwood numbers variation.

Figure 12 shows the evolution of the average Nusselt and Sherwood numbers with undulation number n.

By increasing the undulation number n from 0 to 3, a slight increase in average Nusselt and Sherwood numbers was noticed. At n = 3 to 9, the numbers' Nu_{avg} and Sh_{avg} decrease with undulation numbers n.

The maximum value of Nu_{avg} and Sh_{avg} is reached at n = 3, while the minimum value is at n = 9 for the two numbers.

The variation of undulation number n does not affect heat and mass exchange rates.

The heat and mass transfer rates have the same value by increasing the undulation number of the wavy horizontal interface.

5 Conclusion

Numerical investigation of bi-dimensional laminar natural convection in a square cavity partially filled with nanofluid and porous medium separated by a wavy interface using the Buongiorno model to resolve differential governing equations based on the Galerkin finite element method was studied. The effects of the Rayleigh number, the amplitude, and the undulation number of the interface on the dynamic and thermal fields reveal that the flow intensity is more significant in the nanofluid layer than in the porous layer by increasing buoyancy forces, which contribute to reinforcing nanofluid circulation in the cavity and enhancing convective heat transfer.

Temperature and concentration nanoparticle distributions are not affected by varying amplitude and undulation number values.

The decline of local, average Nusselt, and Sherwood numbers is not important by increasing amplitude and undulation number values, from which we conclude that the flow is not sensitive to the variation in amplitude and undulation number of the wavy interface.

The present configuration allows for reducing the product development time and costs. And achieving engineering-accurate performance predictions of a specific geometry

This study can be extended to 3-D and incorporate an anisotropic porous medium with variable porosity, hybrid nanofluid, or two- phase fluide using the Buongiorno model.

Acknowledgement:
I would like to thank Mr. Bouzit Mohamed for his support, Mokhefi Abderrahim, and all the elements of the maritime science and engineering laboratory USTO.

Nomenclature

B	thermal expansion coefficient
C	concentration dimensionnel
D_B	Brownian diffusion coefficient
D_T	thermodiffusion coefficient
C_P	specific heat capacity
Da	Darcy number
g	gravitational acceleration
h	heat transfer coefficient
H	height dimensionless
k	thermal conductivity
K	Permeability
L	characteristic length
Le	Lewis number
Nb	Brownian number
Nr	buoyancy ratio
Nt	thermophoresis parameter
Nu_{avg}	average Nusselt number
Nu_{loc}	local Nusselt number
p	pressure
P	Dimensionless pressure
Pr	Prandtl number
Ra	Rayleigh number
Sh_{avg}	average Sherwood number
Sh_{loc}	local Sherwood number
T	dimensional temperature
u, v	dimensional velocity components
U, V	dimensionless velocity components
W	heat flux density
x, y	dimensional space coordinates
X, Y	dimensionless space coordinates

Greek symbol

v	kinematic viscosity
P	pressure
α	thermal diffusivity
θ	dimensionless temperature
ϕ	volume fraction nanoparticle
φ	dimensionless concentration
Ψ_{max}	stream function

Subscripts

c	cold
h	hot
np	nanoparticles
p	porous medium

References:

[1] Kasaeian A., Eshghi A.T., Sameti M., Kearns D.M. A review on the applications of nanofluids in solar energy systems, *Renewable and Sustainable Energy Reviews*, Vol. 43, 2014, 584-598.

[2] Chamkha A.J., Molana M., Rahnama A., Ghadami F. On the nanofluid Application microchannels, A comprehensive review, *Powder technology*. 332(5).2018.

[3] Ramezanizadeh M., Nazari M.A., Ahmadi M.H., Açikkalp E. Application of nanofluid in thermosyphons: *A review Journal of Molecular Liquids* 272, 2018, 395-402.

[4] Kasaeian A., Daneshazarian R., Mahian O., Kolsi L., Chamkha A.J., Wongwises S., Pop I. Nanofluid flow and heat transfer in porous media: A review of the latest developments, *International Journal of Heat and Mass Transfer*, 107, 2017, 778-791.

[5] Tahmasebi A., Mahdavi M., Ghalambaz M. Local thermal non equilibrium conjugate naturalconvection heat transfer of nanofluids in a cavity partially filled with porous media using Buongiorno's model, *Numerical Heat Transfer, Part A: Applications* 73(4), 2018, 254-276.

[6] Mehryan S., Ghalambaz M., Izadi M. Conjugate natural convection of nanofluids inside an enclosure filled by three layers of solid, porous medium and free nanofluid using Buongiorno's and local thermal non-equilibrium models, *Journal of Thermal Analysis and Calorimetry* 135(2) 1047-1067.

[7] Suresh S., Venkitaraj K., Selvakumar P., Chandrasekar M. Synthesis of Al2O3–Cu/water hybrid nanofluids using two step method and its thermo physical properties, Colloids and Surfaces A: *Physicochemical and Engineering Aspects*, 388(1-3) (2011) 4148.

[8] Mehryan S.A., Kashkooli F.M., Ghalambaz M., Chamkha A.J. Free convection of hybrid Al2O3-Cu water nanofluid in a differentially heated porous cavity, *Advanced Powder Technology* 28(9),2017, 2295-2305.

[9] Ghalambaz M., Mehryan S., Izadpanahi E., Chamkha A.J., Wen D. MHD natural convection of $Cu–Al_2O_3$ water hybrid nanofluids in a cavity equally divided into two parts by a vertical flexible partition membrane, *Journal of Thermal Analysis and Calorimetry*,138(2),2019,1723-1743.

[10] Chamkha A.J., Miroshnichenko I.V., Sheremet M.A. Numerical analysis of unsteady conjugate natural convection of hybrid water-based nanofluid in a semicircular cavity, *Journal of Thermal Science and Engineering Applications,*2017, 9(4): 041004.

[11] Ghalambaz M., Sheremet M.A., Mehryan, S., Kashkooli, F.M., Pop I. Local thermal nonequilibrium analysis of conjugate free convection within a porous enclosure occupied with Ag–MgO hybrid nanofluid, *Journal of Thermal Analysis and Calorimetry* 135(2), 2019, 1381-1398.

[12] Selimefendigil F., Öztop H.F. Conjugate Natural convection in a cavity with different nanofluids on different sides of the partition, *Journal of Molecular Liquids* 216, 2015, 67-77.

[13] Sahoo R.R., Ghosh P., Sarkar J. Performance analysis of a louvered fin automotive radiator using hybrid nanofluid as coolant, *Heat Transfer—Asian Research* 46(7),2016, 978-995.

[14] Gorla R., Siddiqa S., Mansour M., Rashad A., Salah T. Heat source /sink effects on a hybrid nanofluid-filled porous cavity, *Journal of Thermophysics and Heat Transfer* 31(4), 2017, 847-875.

[15] Izadi M., Mohebbi R., Delouei A.A., Sajjadi H. Natural convection of a magnetizable hybrid nanofluid inside a porous enclosure subjected to two variable magnetic fields, *International Journal of Mechanical Sciences*, 151, 2018, 154-169.

[16] Arpino F., Massarotti N., Mauro A. Efficient three-dimensional FEM based algorithm for the solution of convection in partly porous domains, *International journal of heat and mass transfer* 54(21-22), 2011.4495-4506.

[17] Vasseur P., *Wang* C., Sen M. Thermal instability and natural convection in a fluid layer over a porous substrate, *Wärme-und Stoffübertragung*, 24(6), 1989, 337-347.

[18] AL-Srayyih B.M., Gao S., Hussain S.H. Effects of linearly heated left wall on natural convection within a superposed cavity filled with composite nanofluid-porous layers, *Advanced Powder Technology*, 30(1), 2018, 55-72.

[19] Sathe S., Lin W.Q, Tong T. Natural convection in enclosures containing an insulation with a permeable fluid-porous interface, *International journal of heat and fluid flow* 9(4),1988,389-395.

[20] Boulahia Z., Wafik A., Sehaqui R. Modeling of free convection heat transfer utilizing nanofluid inside a wavy enclosure with a pair of hot and cold cylinders, *Frontiers in Heat and Mass Transfer (FHMT),* 8.14, 2017.

[21] Khanafer K., AL-AzmI B., Marafie A., Pop I. Non-Darcian effects on natural convection heat transfer in a wavy porous enclosure, *International Journal of Heat and Mass transfer* ,7–8, 2009, 1887-1896.

[22] Sivasankaran S., Bhuvaneswari M. Natural Convection in a Porous Cavity with Sinusoidal Heating on Both Sidewalls. *Numerical Heat Transfer, Part A: Applications. An International Journal of Computation and Methodology,* 63, 2012, 14-30.

[23] Sheremet M., Cornelia R., Pop I. Free convection in a porous wavy cavity filled with a nanofluid using Buongiorno's mathematical model with thermal dispersion effect, *Applied Mathematics and Computation,* 299, 2017:1-15.

[24] Alsabery A., Tayebim T., Chamkha A.J., Hashim I. Natural convection of Al_2O_3-water nanofluid in a non-Darcian wavy porous cavity under the local thermal non-equilibrium condition, *Scientific Reports*,10 (1)2020:1-22.

[25] Alhashash A., Saleh H. Natural convection induced by undulated surfaces in a porous enclosure filled with nanoliquid, *Advances in Mechanical Engineering*, 11(9), 2019, 1-9.

[26] De Lemos, M.J.S., Silva R.A. Laminar Flow Around a Sinusoidal Interface Between a Porous Medium and a Clear Fluid, *IMECE*2003-41452, pp. 283-290.

[27] Benygzer C., Bouzit M., Mokhefi A., Khelif F.Z. Unsteady natural convection in a porous square cavity saturated by nanofluid using Buongiorno Model: Variable permeability effect on hmogeneous porous medium, *CFD letters*, 2022, 14(7):42-61.

[28] Kadhim H.T., Jabbar F.A., Rona A. Cu-Al2O3 hybrid nanofluid natural convection in an in an inclined enclosure with wavy walls partially layered by porous medium, *International Journal of Mechanical Science,*186 (2), 2020,105889.

[29] Aly A.M., Raizah Z.A.S. Mixed Convection in an Inclined Nanofluid Filled-Cavity Saturated With a Partially Layered Porous Medium, *J. Thermal Sci. Eng. Appl*,2019, 11(4):041002.

[30] Mehdaoui R., Elmir M., Mojtabi A. Effect of the Wavy permeable Interface on Double Diffusive Natural Convection in a Partially Porous Cavity, *The International Journal of Multiphysics*, Vol. 4 No. 3, 2010, 217-231.

[31] Bouafia I., Mehdaoui R., Kadri S**.,** Elmir M. Natural Convection in a Porous Cavity Filled with Nanofluid in the Presence of Isothermal Corrugated Source, *International Journal of Heat and Technology* Vol. 38, No. 2, 2020, pp. 334-342.

[32] Alsabery A. I., Tayebi T., Abosinnee A.S ., Raizah Z. A. S., Chamkha A.J., Hashim I. Impacts of Amplitude and Local Thermal Non-Equilibrium Design on Natural Convection within NanoflUid Superposed Wavy Porous Layers, *Nanomaterials* 2021, 11, 1277.

[33] Kadhim H.T., Al-Manea A., Al-Shamani A.N., Yusaf T. Numerical analysis of hybrid nanofluid natural convection in a wavy walled porous enclosure: Local thermal non-equilibrium model, *International Journal of Thermofluids*, 15 (2022) 100190.

[34] Kadhim H.T., Al Dulaimi Z.M., Rona A. Local Thermal Non-equilibrium Analysis of Cu-Al2O3 Hybrid Nanofluid Natural Convection in a Partially Layered Porous Enclosure with Wavy Walls, Journal of Applied and Computational Mechanics 9(3), (2023), 712-727.

[35] Kolsi L., Hussain S., Ghachem K., Jamal M., Maatki C. Double Diffusive Natural Convection in a Square Cavity Filled with a Porous Media and a Power Law Fluid Separate by a Wavy Interface, *Mathematics* 10(7), 2022, 1060.

[36] Javed S., Deb N., Saha S. Natural convection and entropy generation inside a square chamber divided by a corrugated porous partition, *Results in Engineering* 2023,18 (4):101053.

[37] Nishimura T., Kawamura Y., Ozoe H. Numerical analysis of natural convection heat transfer in a square enclosure horizontally or vertically divided into fluid and porous region, *Technol Rep Yamaguchi Univ*, 1991, 4(5):331-344.

[38] Omri M., Jamal M., Hussain S., Kolsi L., Maatki C. Conjugate Natural Convection of a Hybrid Nanofluid in a Cavity Filled with Porous and Non-Newtonian Layers: The Impact of the Power Law Index, *Mathematics* 2022, 10, 2044.

[39] Tuan N.M., ALY A.M., LEE S.W. Effect of a wavy interface on the natural convection of a nanofluid in a cavity with a partially layered porous medium using the ISPH method, *Numerical Heat transfer Application*, 72(1), 2017, 68-88.

[40] Sheikhzadeh G.A., Nazari S. Numerical Study of Natural Convection in a Square Cavity Filled with a Porous Medium Saturated with Nanofluid, *Trans. Phenom. Nano Micro Scales*, 1(2), 2013, 138-146.

Contribution of Individual Authors to the Creation of a Scientific Article (Ghostwriting Policy)

The authors equally contributed to the present research, at all stages from the formulation of the problem to the final findings and solution.

Sources of Funding for Research Presented in a Scientific Article or Scientific Article Itself

No funding was received for conducting this study.

Conflict of Interest

The authors have no conflicts of interest to declare.

APPENDIX

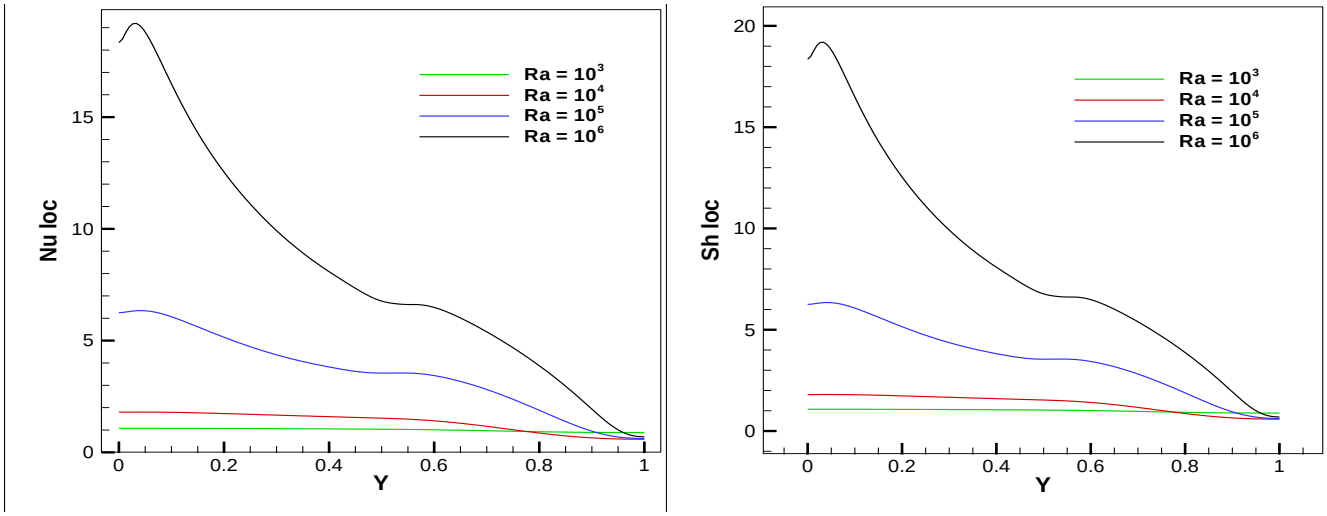

(a) (b)

Fig. 7: Local Nusselt and Sherwood numbers as a function of Ra

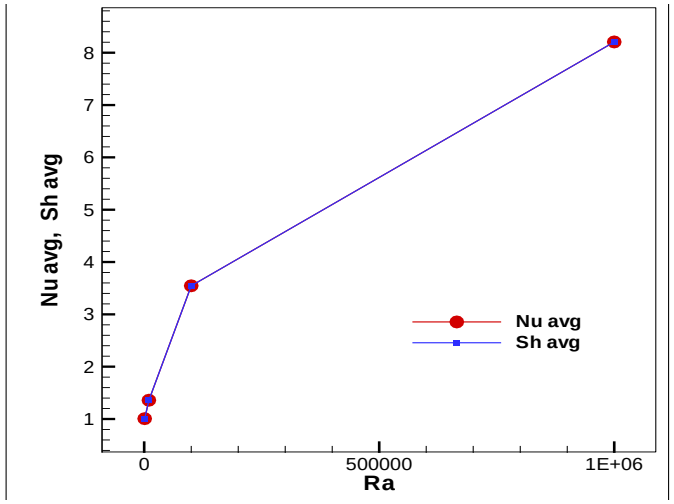

Fig. 8: Average Nusselt and Sherwood numbers as a function of Ra

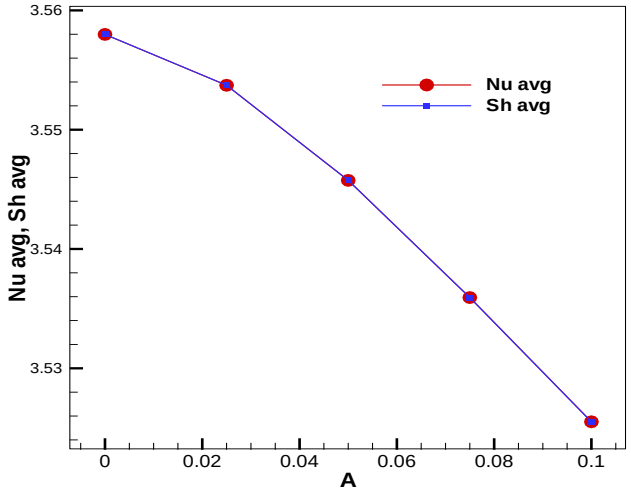

Fig. 9: Average Nusselt and Sherwood numbers as a function of A

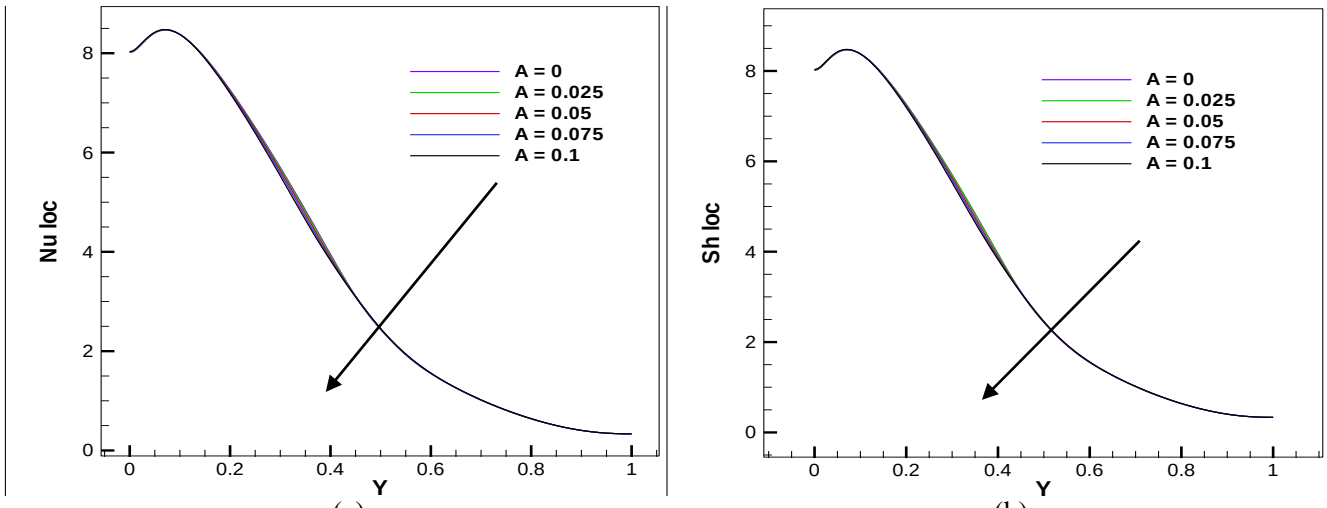

(a) (b)

Fig. 10: Local Nusselt and Sherwood numbers as a function of A

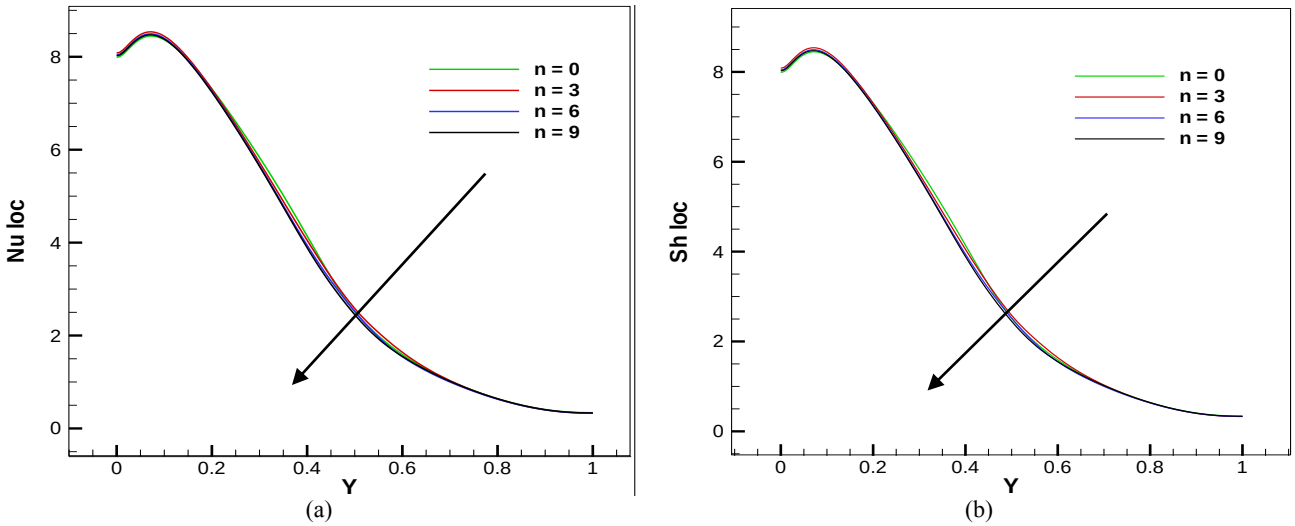

(a) (b)

Fig. 11: Local Nusselt and Sherwood numbers as a function of n

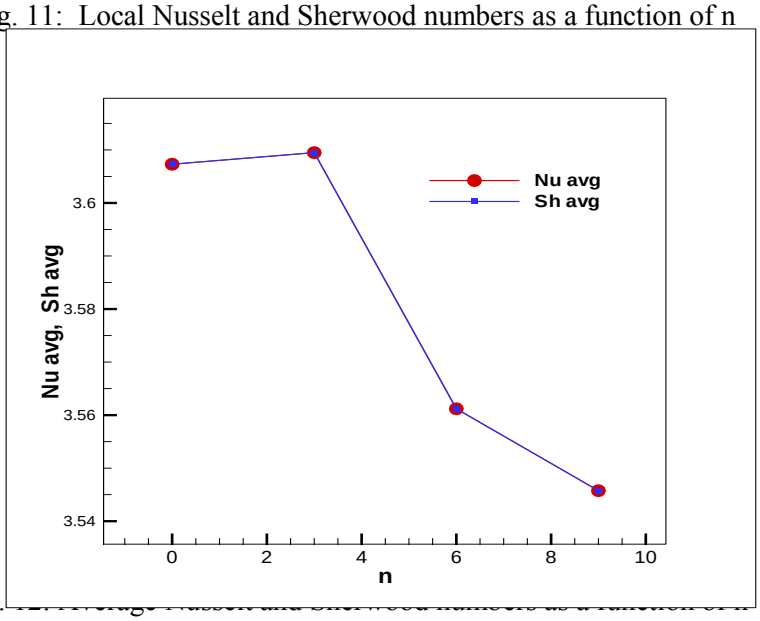

Fig. 12: Average Nusselt and Sherwood numbers as a function of n